

Fault Location Using Sparse L_1 Estimator and Phasor Measurement Units

A. Mouco, A. Abur

Abstract—This paper presents an approach which allows system-wide fault location using only a sparse set of synchronized phasor measurements. The proposed algorithm combines a fault location method using sparse estimation and post-fault voltage prediction. The resulting method enables practical application of the sparse estimation formulation by using Prony analysis to predict post-fault steady state voltages at those buses equipped with phasor measurement units. The prediction requires only a short transient recording which is typically available before the operation of the protective relays. Following the prediction step, the least angle regression based sparse estimation algorithm is employed in order to identify the fault location. A 3ϕ model of the IEEE 118 bus system is developed on the alternative transients program, in order to simulate realistic fault transients and test the performance and accuracy of the proposed fault location method.

Keywords—Fault location, PMU, sparse estimation, Prony analysis, voltage estimation.

I. INTRODUCTION

Reliability is a major concern for power systems operation. Faults on transmission and distribution lines occur frequently. They can occur due to a wide variety of causes and may have significant financial impacts. Therefore fast and accurate fault location is commonly recognized as one of the most crucial problems in power systems operation [1]. It avoids time consuming inspection and identification of faulted section along long transmission lines, a particularly problematic procedure for underground distribution systems. An accurate and reliable fault location system can reduce financial losses and accelerate service restoration times on shed loads.

Many methods have been proposed for fault location in the literature. They can be broadly classified as those based on traveling waves (e.g. [2] and [3]) or based on effective impedance calculations (e.g. [4] and [5]). Both methods are costly and demand dedicated infrastructure on the transmission or distribution systems. Practical application of other alternative methods, such as those employing artificial intelligence techniques (e.g. [6] and [7]) are generally limited due to their heavy computational requirements.

Phasor measurement units (PMUs) have been heavily deployed on large power systems (noticeably China, United States and India) on the last decades (e.g. [8] and

[9]). PMUs conveniently provide synchronized voltage and current phasor measurements on transmission and distribution systems. Alongside the conventional supervisory control and data acquisition (SCADA) measurements, they increase redundancy, observability, reliability and general situational awareness in real time operation.

It has already been shown that the wide-area fault location can be formulated as a sparse optimization problem. It exploits sparsely located synchronized voltage phasor measurements to efficiently and accurately obtain the location of faults anywhere in the system, regardless of fault type. This fault location approach requires both the pre-fault and post-fault steady state voltages at those few buses equipped with PMUs. While the pre-fault steady state voltages can be readily provided by PMUs, post-fault steady state voltages are not as easily acquired. Typically, fast operating protective relays isolate the faulted line section long before the post-fault steady state is reached.

Control and protection systems, continuously monitor major lines for faults. Once a fault is detected, fast acting relays send trip signals to designated circuit breakers which isolate the fault. This event usually occurs in a few cycles of fundamental frequency. Once circuit breakers operate, they change the system topology. Therefore, the "faulted" steady state voltage will never be allowed to be reached or measured by the PMUs.

PMUs usually sample and record continuous voltage waveforms at a high sampling rate per cycle in order to produce synchronized voltage phasors. The voltage waveform, captured between the time of fault occurrence and the circuit breaker operation, can be used to identify the transfer function model of the system using Prony analysis. This model can then be used to estimate the post-fault steady state voltage.

The proposed algorithm combines and extends the fault location method proposed in [10] and the voltage prediction proposed in [11]. The paper develops a comprehensive approach based on the above observations and tests it using realistic fault scenarios. Simulations on the alternative transients program (ATP), using a 3ϕ model of IEEE 118 Bus system, are used to generate the real-time fault transient recordings to be used by the proposed algorithm. A brief overview of sparse estimation will be given in the next section.

II. SPARSE ESTIMATION

Given an under determined linear system (with more unknowns than available equations) a unique solution can still be found if there is a priori knowledge about the sparse structure of the solution vector. In many engineering applications such situations arise where the solution is

This work made use of Engineering Research Center Shared Facilities supported by the Engineering Research Center Program of the National Science Foundation and the Department of Energy under NSF Award Number EEC-1041877 and the CURENT Industry Partnership Program.

The authors are with the Electrical and Computer Engineering Department, Northeastern University, Boston, MA 02151 USA (e-mail: mouco.a@husky.neu.edu and abur@ece.neu.edu).

Paper submitted to the International Conference on Power Systems Transients (IPST2019) in Perpignan, France June 17-20, 2019.

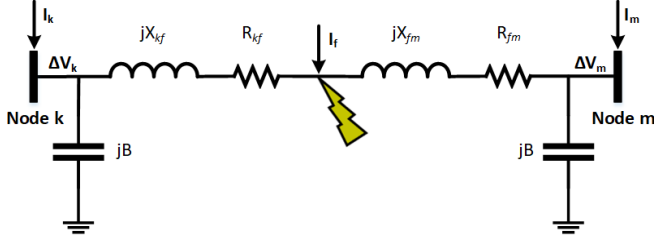


Fig. 1. Bus injection equivalent for fault on transmission line k-m.

expected to have a small number of non-zeros, yet their values are unknown. In those cases, one may be able to recover the sparse solution by using sparse estimation methods as described in [12]. Sparse estimation can be formulated and solved as the following optimization problem:

$$\min_x \|x\|_0 \text{ s.t. } \|y - Ax\|_2 \leq \epsilon \quad (1)$$

where $\|x\|_0$ is the L_0 norm of x and ϵ is the noise associated with the measurement vector y .

It is well known that L_0 minimization is a non-convex, NP-Hard problem (non-deterministic polynomial acceptable problem), and therefore an approximation is necessary to make it computationally efficient. L_1 minimization described in [13], is a convex relaxation of L_0 norm, providing an efficient and naturally robust solution for the sparse problem.

The least absolute shrinkage and selection operator (LASSO) formulation (2) is a constrained version of ordinary least squares (OLS) and presents an interesting solution for such L_1 minimization problems as demonstrated in [12] and [14]:

$$\hat{x}(\lambda) = \arg \min_x \frac{1}{2} \|y - Ax\|_2^2 + \lambda \|x\|_1 \text{ s.t. } \lambda > 0 \quad (2)$$

where $\hat{x}(\lambda)$ is the estimated set of states and λ is the tuning parameter, comprised mostly of zeros, leading to solutions with selective sparsity. The following section provides details of the LASSO algorithm.

A. LASSO Algorithm

The least angle regression (LARS), first proposed by [15], is an algorithm for solving LASSO formulation. The proposed algorithm is an incremental forward stagewise movement with step size tending to zero. One of the most attractive properties of LARS is its computational efficiency, being able to find the sequence of all LASSO solutions, corresponding to varying the regularization parameter λ , at the cost of a single OLS fit.

As demonstrated in [12], the LARS based sparse estimation algorithm can be implemented as:

$$\begin{aligned} \hat{x}(\lambda) &= \arg \min_x f(x, \lambda) \\ \hat{x}(\lambda) &= \arg \min_x \frac{1}{2} \|y - Ax\|_2^2 + \lambda \|x\|_1 \text{ s.t. } \lambda > 0 \end{aligned} \quad (3)$$

Input: $m \times n$ A matrix (Z_{node}), y (ΔV_{node})

Initialize: $x = 0$, $S = \emptyset$, $r = y - Ax = y$

Find the column in A most correlated with residual r :

$$\begin{aligned} i &= \arg \max_i a_i^T r \\ \hat{x}_i &= \max_i a_i^T r \\ S &\leftarrow S \cup \{i\} \end{aligned} \quad (4)$$

Move x_i from 0 toward its least-squares coefficient \hat{x}_{ik} , updating the residuals until some predictor a_j has as much correlation with the current residuals as a_i ; then add it to S .

$$S \leftarrow S \cup \{j\} \quad (5)$$

Move x_i and x_j towards the direction defined by their joint least-squares coefficient (6) until some other predictor a_k has as much correlation with the current residual.

$$\delta_k = (A_{S^k}^T A_{S^k})^{-1} A_{S^k}^T r \quad (6)$$

Then add it to the S :

$$S \leftarrow S \cup \{k\} \quad (7)$$

Continue this process of adding predictors for $(m-1, n)$ steps until full OLS solution is obtained. If $n < m$, all predictors are in the model.

B. Fault Location as a Sparse Estimation Problem

When a power system operating in the normal steady state conditions experiences a disturbance caused by a fault on a transmission line, voltage transients can be observed on all system buses. Considering the hypothetical scenario where there are no protective relays and thus the fault is sustained, this transient will gradually diminish and bus voltages will settle at new post-fault steady state values. Hence, a sustained fault will generate a voltage change on all system buses. Assuming that all system buses are equipped with PMUs, it will be trivial to directly solve for the virtual fault current injections using the equation:

$$Z_{node} * \Delta I = \Delta V \quad (8)$$

where Z_{node} represents the bus impedance matrix, ΔI is the sparse virtual fault current injection vector and ΔV is the vector of voltage changes at system buses due to the fault. Note that unless the fault happens to be at a specific bus, ΔI will have two non-zero entries, corresponding to the faulted line terminal buses for a single phase circuit.

Therefore, having access to all entries of ΔV and solving the equation (8) for ΔI , equivalent current injections at faulted line terminal buses as shown in Fig. 1 can be solved. Fault location along the transmission line can then be determined using the following relation between the equivalent current injections:

$$\begin{aligned} I_k &= I_f \frac{Z_{fm}}{Z_{fm} + Z_{kf}} \\ I_m &= I_f \frac{Z_{kf}}{Z_{fm} + Z_{kf}} \end{aligned} \quad (9)$$

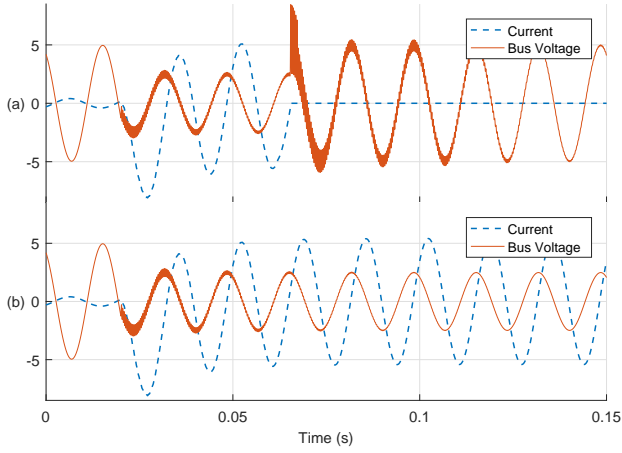


Fig. 2. Fault on transmission line with protection actuation (a) and without protection actuation (b).

consequently:

$$Fault\ Location(m) = \frac{I_k}{I_k + I_m} * 100\% \quad (10)$$

$$Fault\ Location(k) = \frac{I_m}{I_k + I_m} * 100\%$$

where I_k and I_m represent the equivalent fault current injections at buses k and m , respectively. Z_{kf} and Z_{fm} represent the equivalent impedance between the terminal nodes and the fault point.

Unfortunately, in a typical power system only a small percentage of the buses have PMUs. Thus, equation (8) will be under determined and solution for ΔI will not be possible. However, since it is known a priori that the solution will contain at most six non-zero entries, considering the case of a 3ϕ to ground fault, sparse estimation can be used to identify the correct ΔI vector, even when only a small subset of entries of ΔV are available.

Since the LARS algorithm cannot directly process complex numbers, the network equation given by (8) is transformed into a set of real equations as follows:

$$\begin{bmatrix} \Re(Z_{node}) & -\Im(Z_{node}) \\ \Im(Z_{node}) & \Re(Z_{node}) \end{bmatrix} * \begin{bmatrix} \Delta\Re(I_{node}) \\ \Delta\Im(I_{node}) \end{bmatrix} = \begin{bmatrix} \Delta\Re(V_{node}) \\ \Delta\Im(V_{node}) \end{bmatrix} \quad (11)$$

where \Re and \Im denotes the real and imaginary parts of a complex number, respectively.

The remaining issue is to obtain accurate measurements of pre-fault and post-fault bus voltages at those few buses with PMUs. After the fault is detected by the relays, it is usually cleared by circuit breakers after a few cycles. Once the topology changes, the following steady state voltages provided by the PMUs will no longer reflect the post-fault conditions, hence cannot be used by the proposed algorithm. Since PMUs are not able to readily provide the post-fault steady state voltage due to the fast acting relays that clear the fault, these values need to be estimated by a separate algorithm. Modern PMUs, however, can capture the voltage transients between the

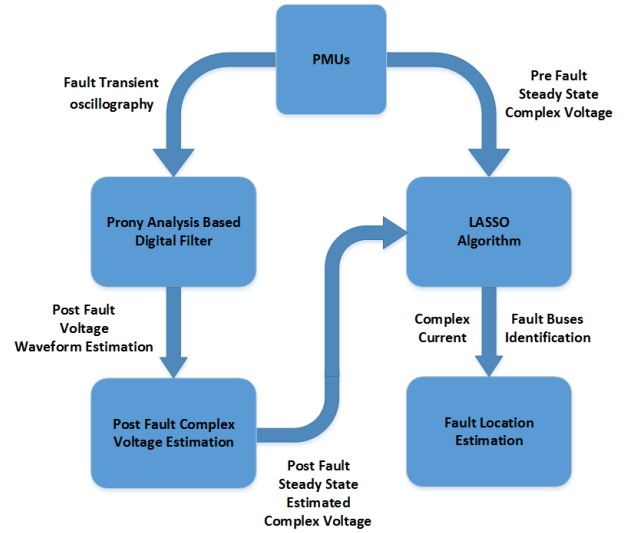


Fig. 3. Sparse Estimation Based Fault Location - Flowchart

fault occurrence and clearance. This information can be used to estimate the post-fault steady state voltage, as described in the next section.

III. POST FAULT STEADY STATE ESTIMATION

This section describes the use of Prony analysis in order to estimate the post-fault steady state bus voltages from a recording of the same bus voltage during the first few cycles of fault transients, before the relays operate and clear the fault. As mentioned, after the fault is isolated the steady state voltage measurements cannot be used for the fault location estimation formulation, since they represent a different system topology. However, the post-fault steady state voltage can be estimated. An example of a bus voltage profile, considering the incidence of a system fault, with and without protection actuation can be seen in Figs. 2(a) and 2(b) respectively.

Modern PMUs have the capability of, not only providing synchronized voltage and current angles and magnitudes, but also recording high frequency transients of those quantities for analysis purposes. As demonstrated in [11], it is possible to use such recorded transients to estimate the post-fault steady state voltage. This estimation is based on Prony Analysis, a deterministic exponential model that provides the best performance for modeling power system transients when compared with other available techniques (e.g. Fourier transform, auto regressive or auto regressive moving average models) [16].

The proposed digital filter is based on the identification of a transfer function that represents accurately the time-domain response of a given system [17]. The input signal is analyzed and the following mathematical procedure yields the desired transfer function:

$$H(z) = \sum_{n=0}^{\infty} h(n)z^{-n} \quad (12)$$

where $h(n)$ is the impulse response related to $H(z)$ by the z transform. It can also be described as a transfer function:

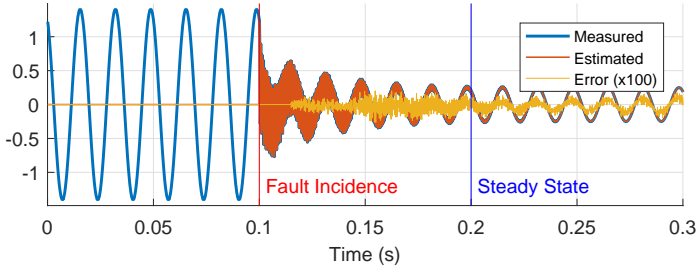


Fig. 4. Voltage Estimation Result - Bus 100 - Phase A - 3ϕ to ground Fault

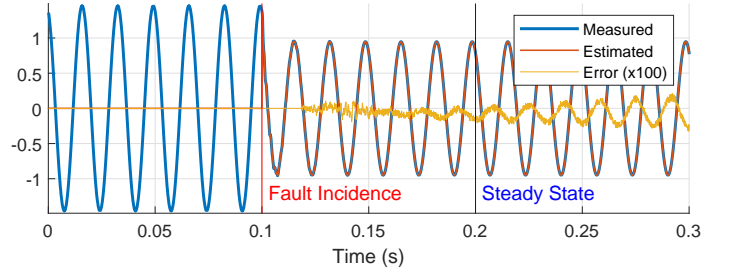


Fig. 6. Voltage Estimation Result - Bus 49 - Phase A - 3ϕ to ground Fault

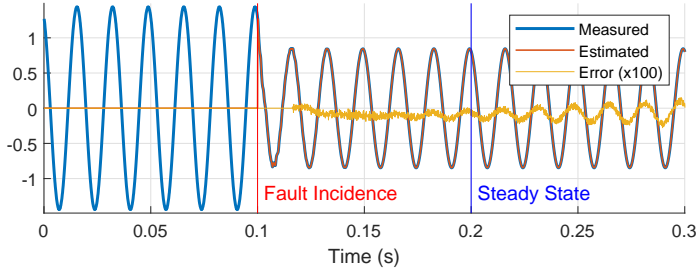


Fig. 5. Voltage Estimation Result - Bus 100 - Phase A - ϕ to ϕ Fault

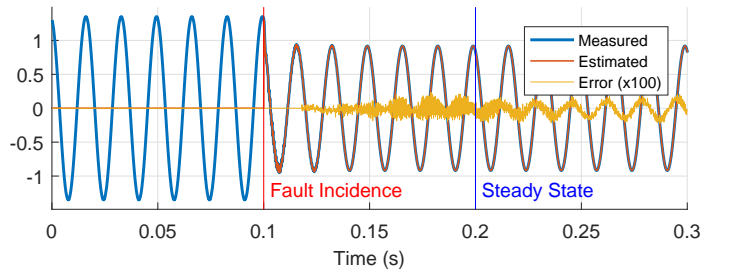


Fig. 7. Voltage Estimation Result - Bus 56 - Phase A - ϕ to ground Fault

$$H(z) = \frac{B(z)}{A(z)} = \frac{b_0 + b_1 z^{-1} + b_2 z^{-2} + \dots + b_m z^{-m}}{1 + a_1 z^{-1} + a_2 z^{-2} + \dots + a_n z^{-n}} \quad (13)$$

where B represent the m zeros and A represent the n poles of the transfer function $H(z)$. The above equation can also be written as:

$$B(z) = H(z) * A(z) \quad (14)$$

As a matrix product, the first $k + 1$ terms of the impulse response can be expressed as:

$$\begin{bmatrix} b_0 \\ b_1 \\ b_2 \\ \vdots \\ b_m \\ 0 \\ \vdots \\ 0 \end{bmatrix} = \begin{bmatrix} h_0 & 0 & 0 & \dots & 0 \\ h_1 & h_0 & 0 & & \vdots \\ h_2 & h_1 & h_0 & \dots & \vdots \\ \vdots & & & \ddots & \vdots \\ h_m & \vdots & & & \vdots \\ \vdots & \vdots & & & \vdots \\ h_k & & & & h_{k-m} \end{bmatrix} \cdot \begin{bmatrix} 1 \\ a_1 \\ a_2 \\ \vdots \\ a_n \end{bmatrix} \quad (15)$$

or in a simplified form:

$$\begin{bmatrix} b \\ \dots \\ 0 \end{bmatrix} = \begin{bmatrix} \dots & H_1 & \dots \\ \dots & \dots & \dots \\ h_{21} & \vdots & H_2 \end{bmatrix} \cdot \begin{bmatrix} 1 \\ \dots \\ a^* \end{bmatrix} \quad (16)$$

where b is the vector of $m + 1$ numerator coefficients, a^* is the vector of n denominator coefficients, with $a(0) = 1$. This format of H matrix is used to simplify the transfer function calculation as:

$$0 = h_{21} + H_2 \cdot a^* \quad \text{or} \quad h_{21} = -H_2 \cdot a^* \quad (17)$$

and

$$b = H_1 \cdot a \quad (18)$$

where a^* and b yields, respectively, the denominator and numerator coefficients of the transfer function (13). This mathematical procedure provides a transfer function equivalent model based on sample data. This model can be used to estimate the behavior of the system.

IV. SIMULATIONS

In order to evaluate the proposed algorithm, a test system is modeled in ATP, providing representative voltage transient waveforms of fault occurrence and protection actuation. The selected sparse set of synchronized waveforms are, thereafter, submitted to the Prony analysis algorithm to calculate the post-fault steady state voltages, as described in Section III. Along with the pre-fault steady state voltages, directly measured by PMUs, the post-fault estimated voltages make it possible to calculate the corresponding entries of the vector ΔV_{node} , whose dimension will typically be quite small compared with the system size. Extracting the corresponding rows of Z_{node} and using the sparse estimation algorithm discussed in Section II the equivalent fault current injections are estimated. Fault location can then be calculated using (10). A flowchart of the overall fault location procedure is shown in Fig. 3.

A. Test System

The positive sequence newtork model of the IEEE 118-bus system is expanded to a full detailed 3ϕ model. ATP is used to provide both pre-fault steady state and fault transient voltage waveforms. Note that the 3ϕ transmission lines are modeled with their self and mutual impedances. Line charging is also considered. All transformers (modeled as Wye-Wye

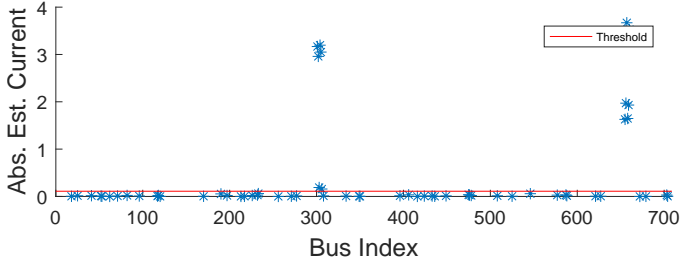


Fig. 8. Sparse Estimation Result - Fault at 50% of Line 101-102 - 3ϕ to ground

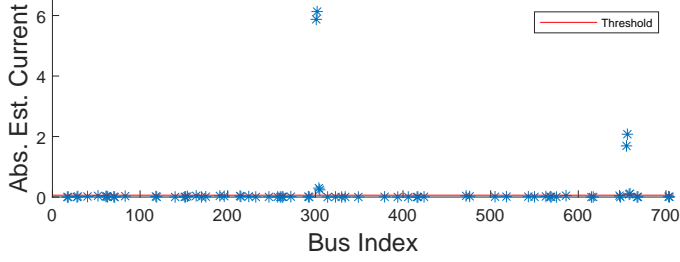


Fig. 9. Sparse Estimation Result - Fault at 5% of Line 101-102 - ϕ to ϕ

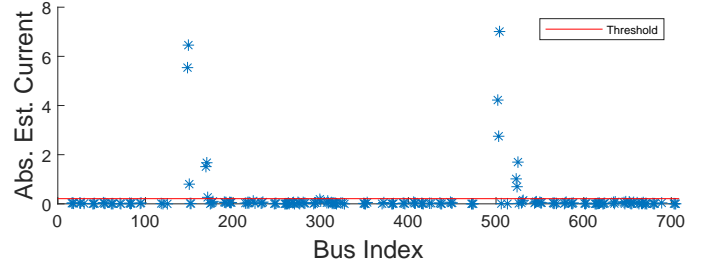


Fig. 10. Sparse Estimation Result - Fault at 20% of Line 50-57 - 3ϕ to ground

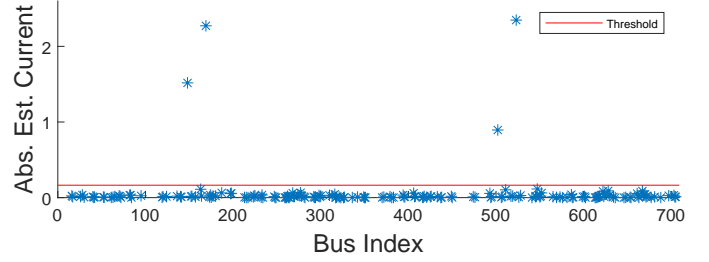


Fig. 11. Sparse Estimation Result - Fault at 65% of Line 50-57 - ϕ to ground

grounded), capacitors, reactors and loads are also represented, providing adherence the unifilar model.

The 3ϕ voltage waveforms, provided by ATP, are captured between the fault application and the circuit breaker actuation using a time step of $0.1ms$. According to [11], this resolution optimizes the process, providing enough information for accurate estimation without burdening the analysis with high frequency transients, whose influence on the estimator results is negligible and can be conveniently disregarded.

It is shown in [11] that 1.5 cycles of fundamental frequency provided enough information to predict the post-fault steady state voltage with less than 1% of error for all the simulated scenarios. It is also shown that the more cycles are used the more accurate will be the prediction. The simulations presented in the next section consider 3 cycles of fundamental frequency between the occurrence and clearing of the fault. According to [18], this is a conservative assumption for fault clearance considering the available technology of today's protection systems. In the following simulations, the discrepancy between the estimated and true post fault voltages obtained using 3 cycles of information is found to be less than 0.1%.

The post fault steady state estimator, discussed in Section III, uses a total of 18 cycles of voltage waveform data for all buses and phases selected. The first 6 cycles are measured, used to compute the pre-fault steady state voltage, since the fault is applied at the beginning of the 7th cycle with respect to a reference sine wave. As mentioned above, 3 cycles of transients, measured right after the fault, are used to estimate 12 cycles of the post-voltage waveforms. The first 6 estimated cycles are discarded in order to avoid errors caused by fault transients, and the last 6 cycles are used to estimate the post-fault steady state voltage. Those voltages are then subtracted to provide the voltage difference caused by the fault. Note that both pre and post-fault voltage waveforms

are compared to a reference sine wave ($1\angle 0^\circ$) in order to accurately determine the voltage angle.

B. Simulated Scenarios

The proposed algorithm for fault location is tested by simulating faults at various locations in the 3ϕ IEEE 118 bus system ATP model. Three types of faults are considered: 3ϕ to ground, ϕ to ground and ϕ to ϕ . Note that in Figs. 8 to 11 all results are referred to a bus index as follows:

$$Bus\ Index = [\{b_A\ b_B\ b_C\}_i^{real}, \{b_A\ b_B\ b_C\}_i^{imag}] \quad (19)$$

for $i = 1, \dots, n$.

where n refer to the total number of buses in the system.

For all presented simulations, three phase voltage measurements are assumed to exist at randomly selected 31 buses out of the 118 total buses. As shown in [10], it is possible to check the uniqueness of solution of the sparse estimation algorithm for a given set of measured buses. Note that terminal buses of lines with simulated faults are intentionally excluded from the set of measured buses. Tables I to IV present the estimated fault current and fault location calculations, based on (10), for all the simulated scenarios.

1) *Fault Along Line 101 – 102*: Two scenarios are created on line 101 - 102 where a 3ϕ to ground and a ϕ to ϕ fault are simulated at 50% and 5% of the line length, respectively. Estimated post fault voltages, at measured buses close to the fault, can be seen in Figs. 4 and 5. Determined fault locations are shown in Figs. 8 and 9. Numerical results are also given in Tables I and II.

2) *Fault Along Line 50 – 57*: Similar to the above case, a 3ϕ to ground and a ϕ to ground fault are simulated at 20% and 65% of the line length respectively, along line 50 – 57. Estimated post fault voltages, at measured buses close to the fault, are shown in Figs. 6 and 7. Determined fault locations

TABLE I
ESTIMATOR RESULT - FAULT AT 50% OF LINE 101-102 - 3ϕ to ground

Bus	Phase	Est. Current	Est. Fault Location
101	A	$3.1680 - 1.6288i$	50.23%
101	B	$-2.9593 - 1.9708i$	50.39%
101	C	$-0.1888 + 3.6698i$	48.99%
102	A	$3.1964 - 1.6470i$	49.77%
102	B	$-3.0505 - 1.9312i$	49.62%
102	C	$-0.1569 + 3.5260i$	51.01%

TABLE II
ESTIMATOR RESULT - FAULT AT 5% OF LINE 101-102 - ϕ to ϕ

Bus	Phase	Est. Current	Est. Fault Location
101	A	$5.8731 - 1.6913i$	4.80%
101	B	$-6.1302 - 2.0764i$	3.93%
102	A	$0.2956 - 0.0875i$	95.20%
102	B	$-0.2402 - 0.1105i$	96.10%

TABLE III
ESTIMATOR RESULT - FAULT AT 20% OF LINE 50-57 - 3ϕ to ground

Bus	Phase	Est. Current	Est. Fault Location
50	A	$5.5416 - 4.2220i$	20.74%
50	B	$-6.4571 - 2.7499i$	20.52%
50	C	$0.8004 + 7.0102i$	19.58%
57	A	$1.5136 - 1.0149i$	79.29%
57	B	$-1.6724 - 0.6971i$	79.48%
57	C	$0.2637 + 1.6973i$	80.43%

TABLE IV
ESTIMATOR RESULT - FAULT AT 65% OF LINE 50-57 - ϕ to ground

Bus	Phase	Est. Current	Est. Fault Location
50	A	$1.5151 - 0.8897i$	65.65%
57	A	$2.2741 - 2.3604i$	35.20%

are shown in Figs. 10 and 11 and corresponding numerical results are provided in Tables III and IV.

C. Discussion of Results

Results from the proposed algorithm, presented in Tables I to IV strongly confirm the capability of the method to accurately estimate the location of different types of faults in the simulated scenarios. Note that the estimation remains rather insensitive against noise generated by the Prony based post-fault voltage estimation algorithm, as evident in Figs. 4 to 7. As evident from Figs. 8 to 11 the sparse estimation algorithm yields a few non-zero current injections at buses not incident to faulted line. Fortunately, these can be easily filtered using an appropriate noise threshold as indicated by the red lines in the figures. The thresholds are typically system dependent and can be empirically determined.

V. CONCLUSIONS

This paper presents a wide-area fault location sparse estimator. It uses pre-fault synchronized voltage measurements from PMUs installed at a small number of system buses, post-fault steady state voltages that are predicted using Prony analysis and few cycles of transient voltage recordings captured after the fault occurrence, also provided by PMUs. The objective is to develop a fast and reliable fault

location procedure, and to accomplish this without additional investments on hardware.

The paper contains simulation results that consistently show accurate fault location, with errors in the order of 1% for different types of faults and locations. They illustrate that the proposed algorithm is insensitive to fault type, flexible and can be conveniently implemented in any transmission or distribution system, provided that a sparse set of PMUs and an accurate network model are available.

For future work, the intention is to validate the proposed fault location algorithm using measurements recorded during actual fault incidents.

REFERENCES

- [1] M. M. Saha, J. J. Izykowski, and E. Rosolowski, *Fault location on power networks*. Springer Science & Business Media, 2009.
- [2] P. Gale, P. Crossley, X. Bingyin, G. Yaozhong, B. Cory, and J. Barker, "Fault location based on travelling waves," in *Developments in Power System Protection, 1993., Fifth International Conference on*. IET, 1993, pp. 54–59.
- [3] M. Korkali, H. Lev-Ari, and A. Abur, "Traveling-wave-based fault-location technique for transmission grids via wide-area synchronized voltage measurements," *IEEE Transactions on Power Systems*, vol. 27, no. 2, pp. 1003–1011, 2012.
- [4] T. Kawady and J. Stenzel, "A practical fault location approach for double circuit transmission lines using single end data," *IEEE transactions on power delivery*, vol. 18, no. 4, pp. 1166–1173, 2003.
- [5] M. Kezunovic and B. Perunicic, "Automated transmission line fault analysis using synchronized sampling at two ends," in *Power Industry Computer Application Conference, 1995. Conference Proceedings., 1995 IEEE*. IEEE, 1995, pp. 407–413.
- [6] L. S. Martins, J. Martins, C. Alegria, and V. F. Pires, "A network distribution power system fault location based on neural eigenvalue algorithm," in *Power Tech Conference Proceedings, 2003 IEEE Bologna*, vol. 2. IEEE, 2003, pp. 6–pp.
- [7] R. Mahanty and P. D. Gupta, "Application of rbf neural network to fault classification and location in transmission lines," *IEE Proceedings-Generation, Transmission and Distribution*, vol. 151, no. 2, pp. 201–212, 2004.
- [8] N. A. S. Initiative *et al.*, "Naspi 2014 survey of synchrophasor system networks-results and findings," *North American Synchrophasor Initiative (NASPI)*, 2015.
- [9] A. G. Phadke, "The wide world of wide-area measurement," *IEEE Power and Energy Magazine*, vol. 6, no. 5, pp. 52–65, September 2008.
- [10] G. Feng and A. Abur, "Fault location using wide-area measurements and sparse estimation," *IEEE Transactions on Power Systems*, vol. 31, no. 4, pp. 2938–2945, July 2016.
- [11] A. Mouco and A. Abur, "Improvement of fault location method based on sparse pmu measurements," in *2017 North American Power Symposium (NAPS)*, Sept 2017, pp. 1–5.
- [12] I. Rish and G. Grabarnik, *Sparse modeling: theory, algorithms, and applications*. CRC press, 2014.
- [13] I. Barrodale and F. D. Roberts, "An improved algorithm for discrete L_1 linear approximation," *SIAM Journal on Numerical Analysis*, vol. 10, no. 5, pp. 839–848, 1973.
- [14] R. Tibshirani, "Regression shrinkage and selection via the lasso," *Journal of the Royal Statistical Society. Series B (Methodological)*, pp. 267–288, 1996.
- [15] B. Efron, T. Hastie, I. Johnstone, R. Tibshirani *et al.*, "Least angle regression," *The Annals of statistics*, vol. 32, no. 2, pp. 407–499, 2004.
- [16] T. Lobos, J. Rezmer, and H.-J. Koglin, "Analysis of power system transients using wavelets and prony method," in *Power Tech Proceedings, 2001 IEEE Porto*, vol. 4. IEEE, 2001, pp. 4–pp.
- [17] T. W. Parks and C. S. Burrus, *Digital filter design*. Wiley-Interscience, 1987.
- [18] J. C. Smith, G. Hensley, and L. Ray, "Ieee recommended practice for monitoring electric power quality," *IEEE Std*, pp. 1159–1995, 1995.